BEAM LOSS MONITOR SYSTEM FOR MACHINE PROTECTION

B. Dehning, CERN, Geneva, Switzerland

Abstract

Most beam loss monitoring systems are based on the detection of secondary shower particles which depose their energy in the accelerator equipment and finally also in the monitoring detector. To allow an efficient protection of the equipment, the likely loss locations have to be identified by tracking simulations or by using low intensity beams. If superconducting magnets are used for the beam guiding system, not only a damage protection is required but also quench preventions. The quench levels for high field magnets are several orders of magnitude below the damage levels. To keep the operational efficiency high under such circumstances, the calibration factor between the energy deposition in the coils and the energy deposition in the detectors has to be accurately known. To allow a reliable damage protection and quench prevention, the mean time between failures should be high. If in such failsafe system the number of monitors is numerous, the false dump probability has to be kept low to keep a high operation efficiency. A balance has to be found between reliable protection and operational efficiency.

BEAM LOSS MEASUREMENT DESIGN APPROACH

For the design of a safety system, in addition to the standard specifications, like dynamic range, resolution, response time, also a value for the "Mean Time Between Failures" (MTBF) is needed to quantify the level of the protection. The estimate of the MTBF value was based in the case of CERN's LHC on the SIL (Safety Integrity Level) approach [1]. Other approaches like "As Low As Reasonably Practicable" (ALARP) are also often used. For both approaches the MTBF value is estimated by the calculation of the risk of damage and the resulting down time of the equipment [3]. In the case of a failure in the safety system itself, it will fall in a failsafe state with the consequence of making the protected system unavailable.

The design considerations of a beam loss monitor system for machine protection are schematically shown in Figure 1. In the first row the above discussed key words are listed. A risk requires a safety system which provides protection but it also reduces the availability of the protected system. In the risk column the consequences (damage and quench) of a non nominal operation (beam loss) are listed. A further consequence for both is the increase of the downtime of the accelerator. The risk is scaling with the consequences of the proton loss event and its frequency. From the risk the MTBF value is deduced. This main design criterion for the safety system is listed in the safety column as well as the means (failsafe, redundancy, survey, check) to reach the

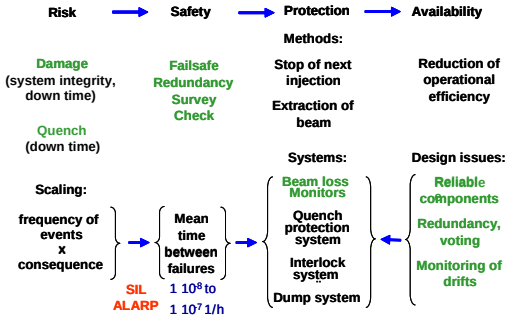

Figure 1: Schematic of the LHC beam loss system design approach (items in green are discussed in this paper).

envisaged MTBF value. In the protection column the methods of protection are listed (stop of next injection and extraction of beam) for a one path particle guiding system (linac, transfer line) and for a multi path system (storage ring). The safety system is consisting of a beam loss measurement system, an interlock system and a beam dump system. In the case of the usage of superconducting magnets, some protection could also be provided by the quench protection system. The availability column lists the means used in the design of the safety system to decrease the number of transitions of the system into the failsafe state. The effect of the components added to the system to increase the MTBF value results in a reduction of the availability of the system. This negative consequence of the safety increasing elements are partially compensated by the choice of reliable components, by redundancy voting and the monitoring of drifts of the safety system parameters (see Figure 1, fourth column). The key words listed in green will be discussed below.

Damage and Downtime

The damage potential at CERN's LHC is over two orders of magnitude higher than at all other existing accelerators (see Figure 2), since the stored beam energy given by the product of the single particle energy and intensity is largest at LHC. The consequence of a dangerous proton loss event was "illustrated" by an accidental loss at Fermi labs Tevatron (200 times lower stored beam energy as at LHC) where the proton beam was lost in a duration of a few revolutions melting some components. The loss was initiated by a moveable measurement instrument. The number of such moveable objects at LHC is also an order of magnitude higher than at Tevatron. This example may indicate the risk associated with the operation of LHC like beams leading to downtimes of months or even years.

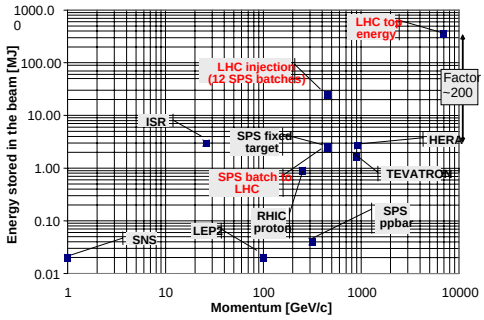

Figure 3: Comparison of the stored beam energy of different high energy physics accelerators as function of the beam momentum.

Quench of Magnets and Downtime

The proton loss initiated quench of magnets is depending on the loss duration and on the beam energy. A quench of a magnet will create a downtime in the order of hours in the case of LHC. To make the operation more efficient the beam could be dumped and a new store prepared. Figure 3 shows the expected loss dependence as

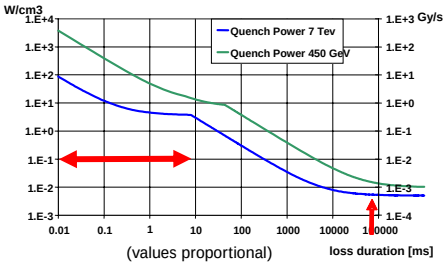

Figure 2: LHC bending magnet quench level curves as function of the loss duration.

function of the loss duration. The two curves indicate the levels for the injection and top energy of LHC. The two arrows indicate loss durations where the quench level of LHC are compared with levels at other storage rings (instant losses, steady state, see Table 1) [6][7]. It can be

Table 1: Instant and steady state loss duration quench levels for different accelerators.

instant (0.01 - 10 ms)	J/cm^3
Tevatron	4.5E-03
RHIC	1.8E-02
LHC	8.7E-04
HERA	2.1 - 6.6E-03

steady state	W/cm^3
Tevatron	7.5E-02
RHIC	7.5E-02
LHC	5.3E-03

seen that the expected quench levels at LHC are lowest, resulting also in advanced requirements for the quench level detection.

The energy dependence of the quench levels is already seen in Figure 3, their dependency as function of energy is shown in Figure 4. The quench levels decrease rapidly with the particle energy leading to the requirement that the quench level threshold need to be decreased during the energy ramp accordingly.

Safety Means

The risk of damage could be reduced by safety means, which are incorporated in the safety system (see Figure 1,

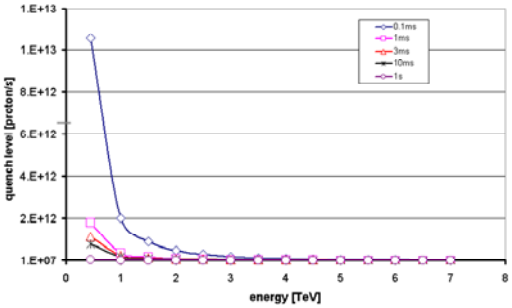

Figure 4: LHC bending magnet quench level curves as function of the beam energy. The parameterisation is for different loss durations.

second column). The most common safety feature of a system is the incorporation of the failsafe mechanism. In case of a failure of the safety system this system falls into a state where the protection is insured. If the system is doubled, redundancy is added, which will reduce the MTBF significantly for short time periods, but tends to reach the same value of the MTBF for long periods (see Figure 5, failure rate = 1/MTBF) [4]. The use of a redundant and surveyed system will decrease the MTBF

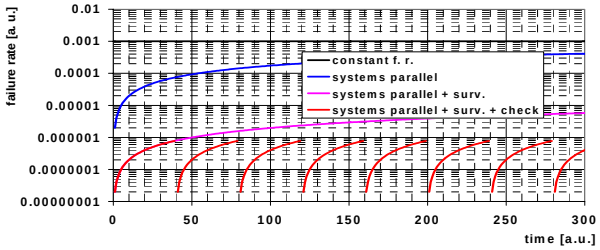

Figure 5: Calculation of the failure rates ranging from a simple system to redundant systems with surveillance and checks.

value for all durations compared to the simple redundant system. An even better result could be reached when a parallel system is not only surveyed but also its functionally is tested during the operation. This procedure will allow to assume that the status of the system after the test is identical to the status of the system as new. The frequency of the test will therefore determine the MTBF value.

Beam Dump Request Distribution

The beam loss measurement system is part of the equipment protection system. The protection as foreseen for LHC is schematically shown in Figure 6 [5]. The number of beam dump request, which reaches the dump system over the machine interlock, is to 60 % operator initiated request (inspired distribution by HERA [7]). The remaining dump requests are to 30 % caused by beam loss initiated dumps and to 10 % by various other reasons. The beam initiated requests are equally subdivided in losses with a duration below 10 ms and above. The short losses can only be detected by the beam loss system. The long losses can be detected in addition with the quench

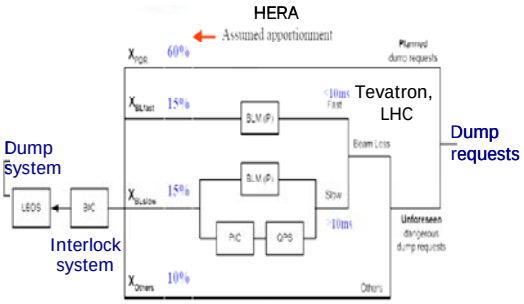

Figure 6: Dump request distribution and the employment of the beam loss system.

protection system (QPS, PIC). In this case two independent systems are available for the detection.

THE BEAM LOSS MEASUREMENT SYSTEM

The last beam loss system design for proton accelerators was done or is under way at SNS, FNAL Tevatron and CERN LHC. These beam systems are used to protect superconducting equipment (cavities at SNS, and magnets at FNAL and CERN). All designs use ionisation chambers as detectors (see Figure 7); however the digitalisation principles are different. The differences

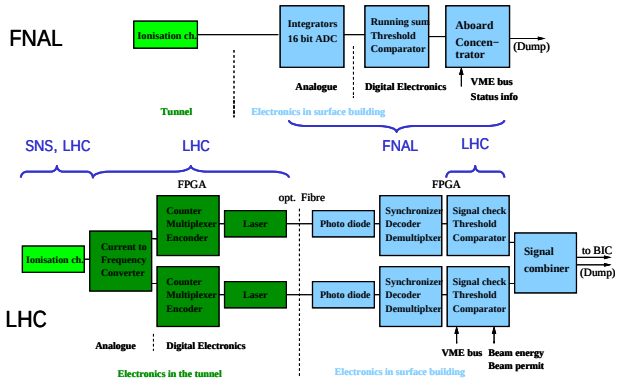

Figure 7: Overview of the beam loss measurement systems at FNAL and LHC. The brackets indicate the discussed subcomponents.

are mainly due to the possible dynamic range. The SNS and FNAL designs use single stage integrators and 24/16 bit ADCs [8][9], whereas the CERN design employs a current to frequency converter (CFC) [10]. The dynamic is about $10^7/10^5$ for the ADCs and 10^8 for the CFC designs. The design of the threshold comparisons in the case of the SNS design is based on analog signal comparisons. The changing thresholds are generated with a DAC. In the case of the FNAL and CERN design the comparison is done digitally in a FPGA. The LHC design is different from the other two in the signal transmission. Due to the extensions of LHC the digitalisation is done near to the detectors and the multiplexed signal from 8 chambers is transmitted over an optical link to the threshold comparator electronic.

Ionisation Chambers

At FNAL, BNL, SNS and CERN mainly ionisation chambers are used for the beam loss detection. At FNAL and CERN chambers are in use which have been designed in the 1970th. For RIC at BNL the FNAL design was copied [11]. For SNS a new design is used, because of the required faster signal response time. A cylindrical stainless steal design with 0.1 litre Ar active volume is used. The signal response limiting ion drift time is reduced from 560 to 72 µs [11]. For LHC a parallel plate design with 1.5 litre N_2 active volume will be used. It is an optimised CERN ISR/SPS design in order to cope with the requested dynamic range of 10^8 and radiation values of 10th of MGy/year in special LHC locations. The lower limit of the dynamic range in the ion chamber is given by the insulation material resistance and the higher limit by the recombination of ions and electrons [12]. The resulting current for the LHC chamber is in the range of a few 10^{-12} to a few 10^{-3} A.

The use of the chamber outside the beam vacuum implies that not only the lost particle species will reach the chambers. The proton initiated shower in the wall materials (cryostats) consists mainly of gammas, electrons, muons, pions, protons and neutrons. The signal response for this entire particle ensemble is not linearly scaling with their energy specifically at low particle energies [13]. The shower development could be seen by scanning a small particle beam across the chamber (see Figure 8). The peaks in the measured and simulated signals are due to the particle shower development in the

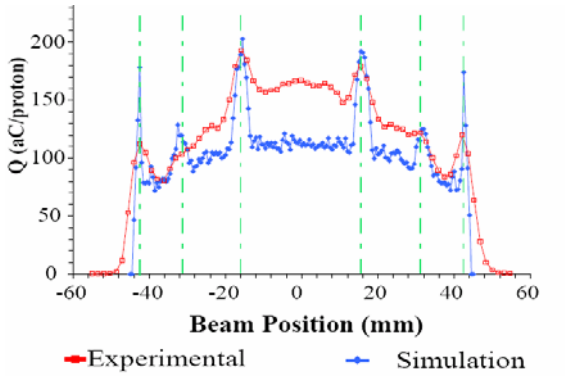

Figure 8: Collected signal charge of a parallel plate ion chamber scanning a proton beam across the chamber.

supporting rots of the parallel electrodes [13].

Another aspect for the usage of ionisation chambers is their high reliability and availability. The chambers used at the CERN SPS operated without failure for 30 years in the ring under an average dose of 0.5 kGy/year and in the injection and extraction areas under a dose of 5 MGy/year. A Cs137 source test of the 142 installed chambers in the SPS ring resulted in a distribution with an average current of 44.7 pA and a width of σ = 1.1 pA. The 41 injection and extraction areas chambers resulted in an average current of 45.5 with a width of σ = 5.8 pA [14]. This example may indicate the low degradation of the

chamber parameters under the influence of radiation and long term employment.

Chamber Signal Integration and Digitalisation

The chamber current integration and digitalisation is done in LHC by a charge balanced integrator (see Figure 9). The input current is converted into a proportional

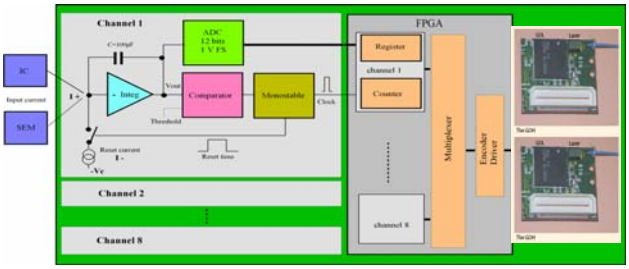

Figure 9: Overview of the LHC chamber signal integration, digitalisation, multiplexing and transmission.

frequency (CFC). To allow a faster response of the CFC for low currents, an ADC was added, which digitalised the integrator output voltage. The CFC frequency is counted over a period of 40 µs and the ADC is read out with the same periodicity. Eight channels are multiplexed, encoded and transmitted using a redundant optical link [10]. The digital signal treatment is done in a radiation tolerant ACTEL FPGA. The whole design is operational up to a total dose of 500 Gy, tested in a 60 MeV proton beam.

Digital Threshold Comparator

The new FNAL and CERN LHC threshold comparators are very similar in their basic design (FNAL see Figure 10). The measured chamber currents are summed over

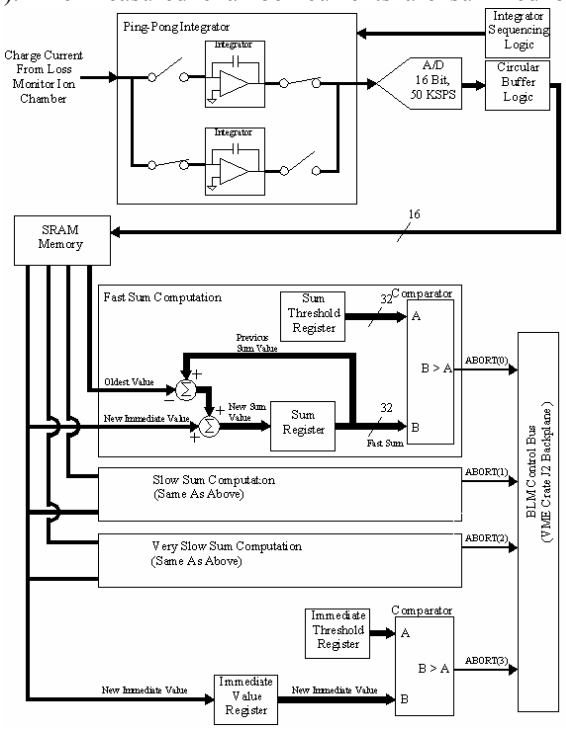

Figure 10: Overview of the FNAL beam loss integration and threshold comparator VME card.

varying periods and compared with corresponding threshold values [9]. The signal from the integrator is treated in different blocks at the same time. In the lower the signal threshold comparison is done for every reading (21 µs) and in the upper a sum is constructed which covers values for 1.4 s (see Table 2). This procedure allows coping with loss duration changing thresholds. Also post-mortem buffers are incorporated in the designs to be able to read out all acquisitions for a certain time period, which were taken before an initialising event (see Table 2).

Table 2: Comparisons of the basic design specifications of the FNAL and CERN LHC threshold comparator cards.

	FNAL	LHC
channels	4	16
Time resolution	21 µs	40 µs
# of running sums	3	11
windows	21 µs to 1.4 s	80 µs to 84 s
thresholds	4	12
Synchronized to machine timing	yes	no
post mortem buffer	4k values	1k values

Redundancy Voting

The redundancy voting procedure allows to increase the availability of a system. An example is the cyclic redundancy check (CRC) comparison of a redundant transmitted signal (see Figure 11). The CRC is calculated

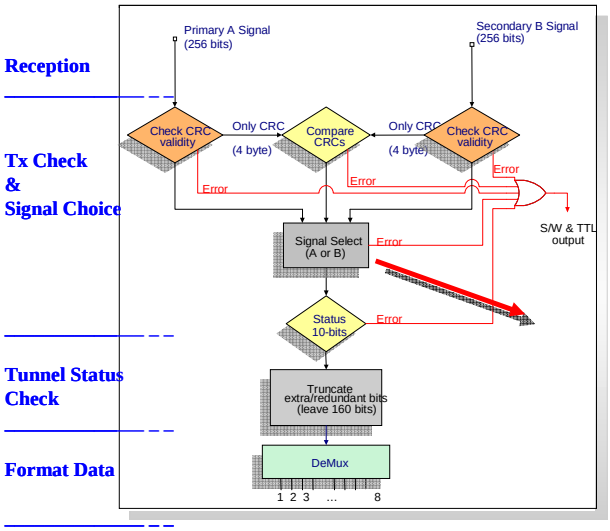

Figure 11: Schematic drawing of the redundant signal transmission comparison for the LHC design.

at the transmitter side and again at the receiver side for each link. For each link the CRCs are compared separately. In addition the CRC of both transmission links, which are calculated at the receiver side, are compared. In case that the comparison of the CRCs of one link is negative, the data of the other link are chosen independently of the result of the CRC comparisons of

both links. The result of the comparison of both links allows to identify the location of the error in the data stream [10].

UNSAFETY OF THE BEAM LOSS SYSTEM

The discussed aim of the beam loss measurement system is the protection of the accelerator equipment to allow an efficient operation. If the detectors are located at the likely loss locations (this aspect is not discussed in this paper), the MTBF value of the beam loss system will indicate the provided safety. This value was calculated for the foreseen LHC beam loss system starting from the single component level and using tabulated or CERN measurements [3][15]. To identify the weakness of safety system components a relative comparison is shown in Figure 12. In the LHC design contributes the ionisation

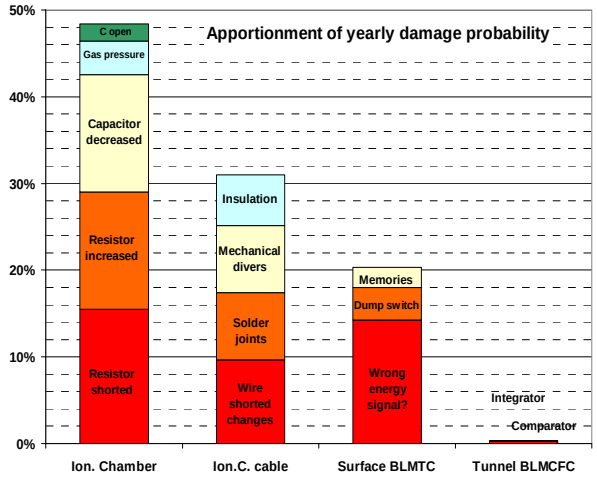

Figure 12: Relative probability of a system component being responsible for a damage to a LHC magnet in the case of a loss.

chambers and their cabling most to the unsafety of the system. Even with no damage in 30 years of the ion chamber operation, systems which are redundant and frequently checked, contribute less to the unsafety. The availability of the system is decreased by false dumps. The components of the beam loss system which are most responsible for this dumps are located in the very front end of the signal treatment chain, which are not redundant. For the LHC design that is the discharge switch of the integrator (see Figure 9).

REFERENCES

[1] "IEC 61508 International Standard", First edition, 1998-12.

[2] G. Guaglio, "Reliability of Beam Loss Monitors System for the Large Hadron Collider", BIW 2004, AIP Conference Proceedings, 10 November 2004 -- Volume 732, Issue 1, pp. 141-149.

[3] G. Guaglio, "Reliability of Beam Loss Monitor Systems for the Large Hadron Collider", Proceeding of ICFA, AIP Conference Proceedings, 8 June 2005, Volume 773, Issue 1, pp. 191-196.

[4] E.B. Holzer, et al., "Design of the Beam Loss Monitoring System for the LHC Ring", 9th European Particle Accelerator Conference EPAC 2004 , Lucerne, Switzerland , 05 - 09 Jul 2004.

[5] R. Filippini et al., "Reliability Assessment of the LHC Machine Protection System", Particle Accelerator Conference PAC 2005, Knoxville, TN, USA, 16 - 20 May 2005.

[6] N. Mokhov, "Protecting Superconducting Magnets from Radiation at Hadron Colliders", Workshop, "Beam generated heat deposition and quench levels for LHC magnets", CERN, 3.-4. March 2005.

[7] K. Wittenburg, "Quench levels and transient beam losses at HERAp", Workshop, "Beam generated heat deposition and quench levels for LHC magnets", CERN, 3.-4. March 2005.

[8] R.L. Witkover and D. Gassner, "Preliminary Design of the Beam Loss Monitoring System for the SNS", AIP Conference Proceedings, 18 December 18 2002, Volume 648, Issue 1, pp. 345-352.

[9] C. Drennan, et al., "Development of a new data acquisition system for the Fermilab beam loss monitors", Nuclear Science Symposium Conference, IEEE, Volume 3, 16-22 Oct. 2004, pp. 1816 – 1819.

[10] C. Zamantzas, et al., "The LHC Beam Loss Monitoring System's Real-Time Data Analysis Card", these proceedings.

[11] R.L. Witkover and D. Gassner, "Design of an Improved Ion Chamber for the SNS", AIP Conference Proceedings, 18 December 2002, Volume 648, Issue 1, p. 337-344.

[12] M. Plum and D. Brown, "Response of Air-Filled Ion Chambers to High-Intensity Radiation pulses", Proceedings of Particle Accelerator Conference, 17-20 May 1993, p. 2181.

[13] M. Hodgson, "Beam Loss Monitor Design Investigations for Particel Accelerators", Depart of Physics, University of Surrey, 15 April 2005.

[14] B. Dehning, "The Beam Loss Monitoring System", 1st LHC Project Workshop, Chamonix 2004, Chamonix, France , 19-23 Jan 2004 – p. 256.

[15] C. Zamantzas, "Beam loss monitors, realisation", LHC Machine Protection Review, CERN, 11-13 April 2005.